

Molecular Analysis of Idiopathic Subglottic Stenosis for *Mycobacterium* Species

Alexander Gelbard, MD; Nicolas-George Katsantonis, MD; Masanobu Mizuta, MD; Dawn Newcomb, PhD; Joseph Rotsinger, MS; Bernard Rousseau, PhD, CCC-SLP; James J. Daniero, MD, MS; Eric S. Edell, MD; Dale C. Ekbom, MD; Jan L. Kasperbauer, MD; Alexander T. Hillel, MD; Liying Yang, MD, MS; C. Gaelyn Garrett, MD; James L. Nettekville, MD; Christopher T. Wootten, MD; David O. Francis, MD, MS; Charles Stratton, MD; Kevin Jenkins, MD; Tracy L. McGregor, MD; Jennifer A. Gaddy, PhD; Timothy S. Blackwell, MD; Wonder P. Drake, MD

Objectives/Hypothesis: Idiopathic subglottic stenosis (iSGS) is an unexplained obstruction involving the lower laryngeal and upper tracheal airway. Persistent mucosal inflammation is a hallmark of the disease. Epithelial microbiota dysbiosis is found in other chronic inflammatory mucosal diseases; however, the relationship between tracheal microbiota composition and iSGS is unknown. Given the critical role for host defense at mucosal barriers, we analyzed tissue specimens from iSGS patients for the presence of microbial pathogens.

Methods: Utilizing 30 human iSGS, 20 intubation-related tracheal stenosis (iLTS), and 20 healthy control specimens, we applied molecular, immunohistochemical, electron microscopic, immunologic, and Sanger-sequencing techniques.

Results: With unbiased culture-independent nucleic acid, protein, and immunologic approaches, we demonstrate that *Mycobacterium* species are uniquely associated with iSGS. Phylogenetic analysis of the mycobacterial virulence factor *rpoB* suggests that, rather than *Mycobacterium tuberculosis*, a variant member of the *Mycobacterium tuberculosis* complex or a closely related novel mycobacterium is present in iSGS specimens.

Conclusion: These studies identify a novel pathogenic role for established large airway bacteria and provide new targets for future therapeutic intervention.

Key Words: Mycobacterium, *Mtb*, idiopathic subglottic stenosis, tracheal stenosis, laryngotracheal stenosis, iSGS, ISS.

Level of Evidence: NA

Laryngoscope, 127:179–185, 2017

Additional supporting information may be found in the online version of this article.

From the Department of Otolaryngology (A.G., N-G.K., M.M., B.R., C.G.G., J.L.N., C.T.W., D.O.F.); the Department of Medicine, Division of Pulmonary and Critical Care (D.N., T.S.B.); the Department of Medicine, Division of Infectious Disease (J.R., J.A.G., W.P.D.); Department of Pathology, Microbiology and Immunology (C.S., K.J.); the Department of Pediatrics, Division of Medical Genetics (T.L.M.C.G.), Vanderbilt University; the Veterans Affairs Tennessee Valley Healthcare Services (J.A.G., T.S.B.), Nashville, Tennessee; the Department of Otolaryngology, University of Virginia Health System (J.J.D.), Charlottesville, Virginia; the Department of Medicine, Division of Pulmonary and Critical Care (E.S.E.); the Department of Otolaryngology (D.C.E., J.L.K.), Mayo Clinic, Rochester, Minnesota; the Department of Otolaryngology, Johns Hopkins (A.T.H.), Baltimore, Maryland; and the Department of Medicine, New York University School of Medicine (L.Y.), New York, New York, U.S.A.

Editor's Note: This Manuscript was accepted for publication April 25, 2016.

Financial Disclosure: Research in North American Airway Collaborative was made possible by infrastructure supported by the Patient-Centered Outcomes Research Institute under award number 1409-22214. We would also like to acknowledge the Vanderbilt genomics core laboratory, Vanderbilt Technologies for Advanced Genomics, supported by an American Recovery and Reinvestment Act (ARRA)-funded National Institutes of Health (NIH) award, as well as the Translational Pathology Shared Resource supported by National Cancer Institute/NIH Cancer Center Support Grant 2P30 CA068485-14. The authors have no other funding, financial relationships, or conflicts of interest to disclose.

Send correspondence to Alexander Gelbard, MD, Assistant Professor, Department of Otolaryngology, Vanderbilt School of Medicine, Medical Center East, S. Tower, 1215 21st Ave. South, Suite 7302, Nashville, TN 37232-8783. E-mail: alexander.gelbard@vanderbilt.edu

DOI: 10.1002/lary.26097

INTRODUCTION

Idiopathic subglottic stenosis (iSGS) is a debilitating extrathoracic obstruction involving the lower laryngeal and upper tracheal airway. It arises without known antecedent injury or associated disease. Emerging study has demonstrated affected patients possess tightly conserved clinical demographics,¹ histopathologic findings,² anatomic injury,³ and physiologic impairment.⁴ Despite description of iSGS more than four decades ago,⁵ only recently has the inflammatory fibrosing phenotype been characterized at the molecular level. Data show highly upregulated activation of the inflammatory IL-17A/IL-23 pathway in the mucosal scar in iSGS, yet the mechanisms responsible for the characteristic demarcated airway inflammation are unknown.

In alternate pulmonary pathologies,^{6–9} both structural and functional changes in the lung epithelium appear to be integral to fibrotic remodeling, occurring in the setting of chronic airway inflammation. Epithelial microbiota dysbiosis, with subsequent sustained host inflammation, is found in other chronic inflammatory mucosal diseases.^{10–18} Although the trachea is lined with respiratory epithelia, which readily support colonization by a diverse microbiome at other upper respiratory sites such as the oropharynx,^{19,20} to date nothing is

known of the composition of the resident microbiome of the large airway or its contribution to airway remodeling in idiopathic subglottic stenosis. Microbiological studies that rely on culture-based techniques underestimate the diversity of species present¹⁰ and offer limited detection of intracellular pathogens. The application of culture-independent approaches offers the opportunity to both provide a broader picture of tracheal microbiome composition and identify discrete pathogenic species associated with disease states.

Previously, work has demonstrated activation of the canonical IL-23/IL-17A pathway in the tracheal mucosa of iSGS patients, and has identified $\gamma\delta$ T cells as the primary cellular source of IL-17A.²¹ Given the established role of $\gamma\delta$ T cell IL-17A in host defense at mucosal barriers, we analyzed tissue specimens from iSGS patients for the presence of microbial pathogens. Our unbiased molecular interrogation of the tracheal microbiota of iSGS patients provides detailed nucleic acid, protein, and immunologic evidence to demonstrate *Mycobacterium* species within tracheal scar. Together with our previous work, these studies offer new insights into the pathogenesis of iSGS. They suggest that human tracheal mucosal health is highly dependent on the composition of the resident microbiota, identify a novel pathogenic role for established large airway bacteria, and offer targets for future therapeutic interventions.

MATERIALS AND METHODS

This study was performed in accordance with the Declaration of Helsinki, Good Clinical Practice, and was approved by the institutional review board (IRB) at Vanderbilt University Medical Center (IRB: 140429).

Patients

In all, 30 iSGS, 20 intubation-related tracheal stenosis (iLTS), and 20 normal control patients were utilized for experiments (Supp. Fig. S1.). Each iSGS and immunoglobulin-like transcripts (iLTS) diagnosis was confirmed using previously described clinical and serologic criteria.²² The control population consisted of patients without known tracheal pathology, malignancy, or systemic infection. Tracheal scar or freshly isolated peripheral blood mononuclear cells (PBMC) was the source of all specimens from the iSGS and iLTS patients, and normal trachea or PBMC was the source for the control patients.

Culture Independent Quantitative Polymerase Chain Reaction Profiling of Respiratory Microbiome

DNA Isolation. Genomic DNA (gDNA) was extracted with the Qiagen DNAeasy extraction kit (Qiagen, Valencia, CA) according to the manufacturer's instructions, with slight modification as previously described.^{23,24} The gDNA concentration and quality were confirmed using the Bioanalyzer 2100 system (Agilent, Santa Clara, CA). Human respiratory pathogen quantitative polymerase chain reaction (qPCR) array (Qiagen) was performed as per manufacturer's instructions in a StepOnePlus instrument (Applied Biosystems, Foster City, CA). Expression analysis was performed using PCR array analysis software (Qiagen).

In Situ Hybridization for Mycobacterial Gene Product GyraseA

Paraffin-embedded iSGS and iLTS airway stenosis tissues and healthy controls (US Biomax Inc., Rockville, MD; # RS321) were pretreated and probed for Gyrase A (Advanced Cell Diagnostics, Hayward, CA, #436701) following a modified RNAscope 2.0 Assay's HD Detection Kit (Red) (Advanced Cell Diagnostics) protocol.²⁵ Tissue was digested with proteinase-K (1:100 dilution) (Sigma-Aldrich Co., LLC. St. Louis, MO) in 20 mM Tris-Cl (p.H. 8.0) for 5 minutes at room temperature. Experimental controls run in parallel included bacterial gene *DapB* as a negative control to assess background signal and *Homo sapiens HS-PPIB* to assess positive signals and protocol efficacy.

Sanger Sequencing of Mycobacterial Species

Molecular subtyping of Mycobacterial Species. Nested PCR analysis was performed as previously described for Mycobacterial *rpoB*²⁶ (with conditions and primers listed in supplemental data [Supp. Table S1]). Negative and positive controls were run in parallel. Genomic DNA extracted from *M. tuberculosis* strain H37rv served as a positive control (Vircell Technologies, Granada, Spain), whereas PCR master mix incubated with 5 μ L of sterile water, and PCR master mix alone were used as negative controls.

Determination of DNA Sequence of Amplified Products

The *rpoB* gene products were run on a 2% gel and purified the 360 bp band using the Qiagen QIAquick Gel Extraction kit (Qiagen) and sequenced directly on both strands in the Vanderbilt Cancer Center Core Sequencing Laboratory, Nashville, Tennessee. Alignments of the *rpoB* sequences were performed using Sequencher 5.3 software (Gene Codes Corporation, Ann Arbor, MI).

Immunogold Labeling

Human tracheal mucosal biopsies were obtained in the operating room and immediately fixed with chilled buffer (50 mM sodium cacodylate [pH 7.4]) containing 2.5% glutaraldehyde and 2.0% paraformaldehyde and placed in 4°C overnight. The samples were then prepared as previously described.²⁷ Briefly, samples were blocked with 0.1% coldwater fish skin gelatin in 50 mM sodium cacodylate buffer and stained with rabbit polyclonal anti-*Mycobacterium tuberculosis* (*Mtb*) antibodies (LS-C72966, LSBio, Inc., Seattle, WA), followed by goat anti-rabbit IgG conjugated to 20 nm gold particles (Electron Microscopy Sciences, Hatfield, PA). Samples were washed three times with phosphate buffered saline containing 0.1% Tween 20 and analyzed with an FEI T-12 transmission electron microscope (FEI, Hillsboro, Oregon) equipped with a side-mounted digital camera. A total of 30 to 35 individual cells in each group were imaged to analyze subcellular architecture and presence of bacteria.

Elispot

Preparation of PBMC and 6-kDa early secreted antigenic target (ESAT-6) peptides,²³ and Elispot assay were performed, as described previously.²⁸ The number of specific interferon gamma (IFN- γ) secreting T cells was calculated by subtracting the mean negative control value from the mean spot-forming cell (SFC) count for duplicate wells inoculated with peptide. Negative controls always had < 50 SFC per 10⁶ input cells. A

positive response was defined as a concentration of at least 50 SFC/10⁶ PBMC, which is at least three times higher than the background level. Research assistants were blind to the clinical diagnoses of the study participants throughout the analysis.

Statistical Analysis

Statistical significance was set at a *P* value less than 0.05, and a mean difference equal to or greater than two-fold change in expression levels. Normal distribution of the variables was tested using the Shapiro-Wilk test. Differences between the *x* and *y* groups were determined using the Kruskal-Wallis and Mann-Whitney tests for normal and nonnormal distributions, respectively. Data were expressed as median ± standard deviation for nonnormal distributed variables. All statistical analyses were performed with Prism version 6.0 software (GraphPad Software Inc., La Jolla, CA).

RESULTS

Culture-Independent Profiling of Respiratory Microbial Flora

Given the role of $\gamma\delta$ T cell IL-17A in host defense against pathogens at epithelial and mucosal barriers, we analyzed tissue specimens from iSGS patients for the presence of microbial species. All iSGS patients (10 of 10) demonstrated PCR positivity to *Mycobacterium* species (Fig. 1A), whereas only two of 10 iLTS patients were positive by PCR (*P* < 0.001). In contrast, among iLTS patients, 10 of 10 showed PCR positivity to *Acinetobacter baumannii* (an established ICU pathogen²⁹), whereas only one of 10 iSGS patients showed a positive signal for this pathogen (*P* < 0.001).

Further confirmatory testing was performed on an additional 10 iSGS, 10 iLTS, and 10 healthy controls with in situ hybridization probing RNA expression of the specific mycobacterial virulence factor DNA gyrase subunit A.³⁰ Seven of 10 iSGS specimens tested positive, predominantly in the tracheal epithelium, whereas only one of 10 iLTS specimens and 0 of 10 healthy control samples showing detectable signal (*P* = 0.03) (Fig. 1B).

Localization of Mycobacterium Species Within iSGS Tracheal Scar

To further investigate for *Mycobacterium* species within tracheal scar tissue, we utilized Immunogold labeling and high-resolution transmission electron microscopy. This analysis revealed multiple structures with associated labels that exhibit typical size (500 nm–2 μ m) and shape (coccoid or bacillus) of *Mycobacterium* species within the extracellular matrix (Fig. 1D-E), whereas controls using secondary antibody alone (data not shown) or an unrelated antibody to *Haemophilus influenzae* (Fig. 1C) were negative. Digital quantification of gold labels per bacterial cell by computerized algorithm confirmed visual analysis of anti-*Mycobacterium tuberculosis* complex (*Mtb*) antibody binding in iSGS tissues (*P* < 0.005) (Supp. Fig. S2).

Systemic Immunologic Response to Mycobacterium Antigens in iSGS

After detection of nucleic and amino acid signal for mycobacteria within iSGS, we sought to assess the systemic immunologic response in iSGS. Utilizing Elispot, we analyzed antigen-specific responses of peripheral leukocytes from iSGS patients to the mycobacterial ESAT-6. We chose ESAT-6 peptides due to prior reports of systemic cellular immune responses to these conserved *Mtb*C virulence factors in sarcoidosis.^{28,31} Peripheral blood mononuclear cells from iSGS patients showed a mean IFN- γ spot-forming-cell (SFC) count of 165.9 (standard error of the mean [SEM] ± 42.4) compared with 27.4 (SEM ± 18.1) in normal controls (*P* < 0.0076) (Fig. 1F). This IFN- γ response suggests systemic immunologic memory to *Mtb*C exposure and is consistent with a pathological role for *Mtb*C in iSGS.

Mycobacterium Species Subtyping via Sanger Sequencing

It was not possible to subtype the *Mycobacterium* species based on the initial primers in our discovery assay; therefore, we utilized Sanger sequencing²⁶ to further classify the *Mycobacterium* species in a subset of samples based on the *rpoB* gene sequence. The *rpoB* PCR yielded a product of 360 bp, which Sanger sequence analysis identified as *Mtb*C in eight iSGS samples. Seven of the eight positive iSGS specimens showed consistent polymorphisms in the same locations (at 2,312 and 2,313 base pairs) (Fig. 2A). Whereas the predicted protein coding sequence from iSGS specimens was homologous to *Mtb* reference sequences (Fig. 2B), phylogenetic analysis of the amino acid sequencing suggests that rather than *Mtb*, a variant member of the *Mtb*C or a closely related novel mycobacterium (Fig. 2C) is present in iSGS specimens.

DISCUSSION

We demonstrate through multiple distinct approaches the presence of *Mycobacterium* within tracheal scar of iSGS patients. Our prior findings suggest a major role for $\gamma\delta$ T cells in the IL-17A-dependent tissue inflammation and fibrotic remodeling seen in the airways of iSGS patients.²¹ Given the established role for $\gamma\delta$ T cells in the early production of IL-17A in *Mtb*C infection,³² and the critical role for IL-17A in host clearance of pulmonary *Mtb*C,³³ our prior results are consistent with our current work demonstrating mycobacterial species within the airway scar of iSGS patients.

An early report describing iSGS as a clinical entity could not isolate bacterial species³⁴ in routine microbiologic culture. Similarly, all iSGS patients included in our study were culture-negative. However, since this publication in 1993, culture-independent techniques have become an established alternate methodology for identification of infectious agents. Polymerase chain reaction was used to identify the etiologic agents of bacillary angiomatosis (*Bartonella henselae*)³⁵ and Whipple's disease (*Tropheryma whippelii*).³⁶

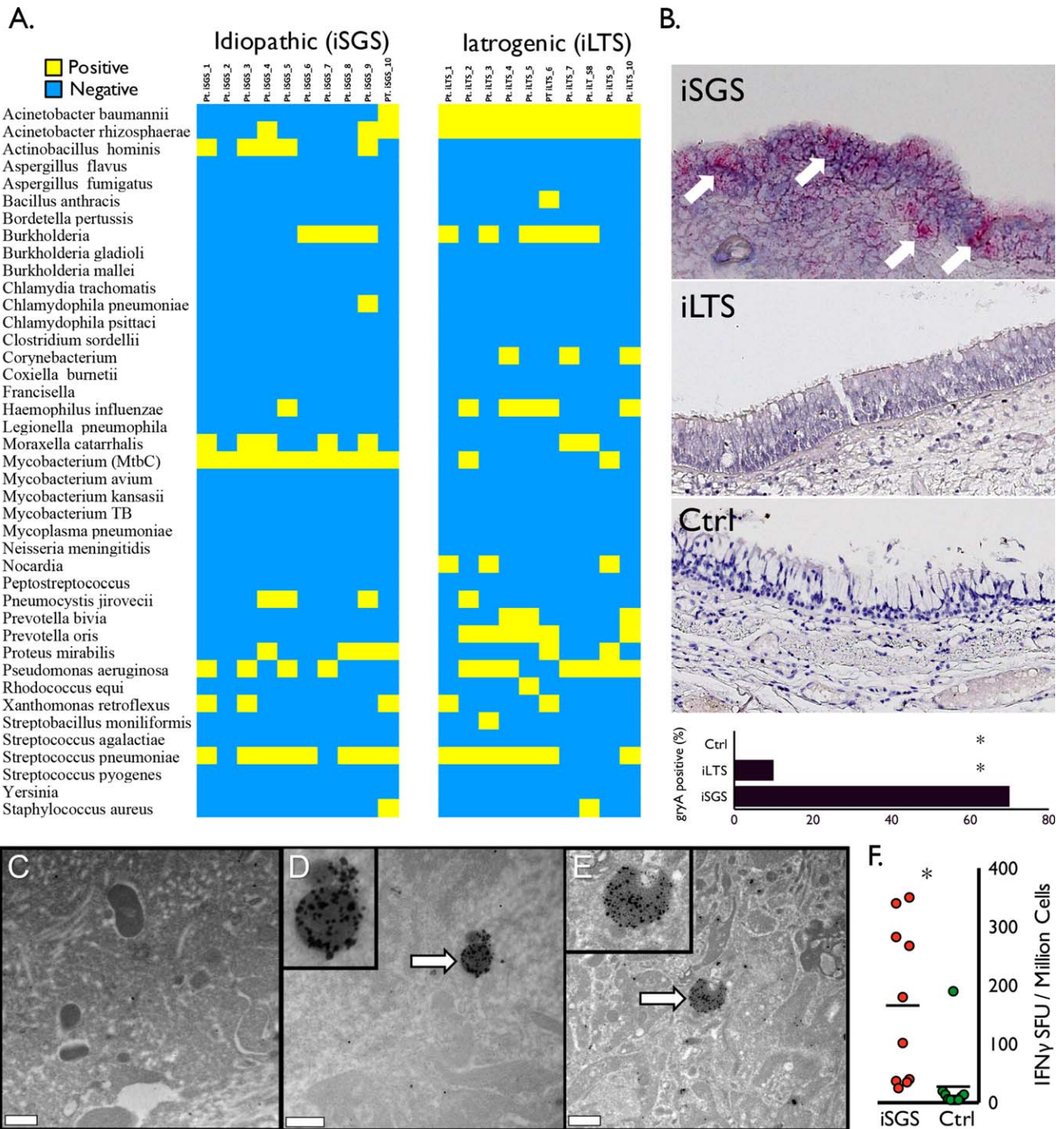


Fig. 1. *Mycobacterium* species in iSGS patients. The qPCR results for panel of respiratory pathogens from 10 iSGS and 10 iLTS patients. (A) Yellow indicates positive PCR products; blue indicates negative result. Ten of 10 iSGS patients had detectable PCR products for *mycobacterium tuberculosis complex (MtbC)*, compared with two of 10 iLTS patients (two-tailed, chi-squared test with continuity correction; $P < 0.001$). (B) Representative images from in situ hybridization for RNA of *Mycobacterium* gene product *gyraseA* (arrows depicting positive signal in iSGS specimen). Accompanying summary graph depicting seven of 10 iSGS patients with detectable in situ hybridization signal, compared with one 10 iLTS and 0 of 10 controls (two-tailed, chi-squared test; asterisk denotes $P < 0.001$). Immunogold labeling with an anti-MtbC antibody and high-resolution transmission electron microscopy analyses revealed multiple structures with associated labels that exhibit typical size (500 nm–2 μ m) and shape (cocci or bacilli) of *Mycobacterium* spp. Treatment with secondary antibody alone (not shown) or an unrelated antibody to *Haemophilus influenzae* (C) revealed sparse labeling that was significantly less than the labeling achieved with the anti-MtbC treatment (D, E). Distribution of IFN- γ production from ESAT-6 stimulated peripheral blood mononuclear cells isolated from the peripheral blood of iSGS patients (red; $n = 10$) or healthy controls (green; $n = 10$). Bars represent the median (50th percentile), asterisk denotes significance (two-tailed, Mann Whitney test; $P < 0.005$) (F). Ctrl = control; IFN- γ = interferon gamma; iLTS = iatrogenic laryngotracheal stenosis; iSGS = idiopathic subglottic stenosis; MtbC = *mycobacterium tuberculosis complex*; PCR = polymerase chain reaction; qPCR = quantitative polymerase chain reaction.

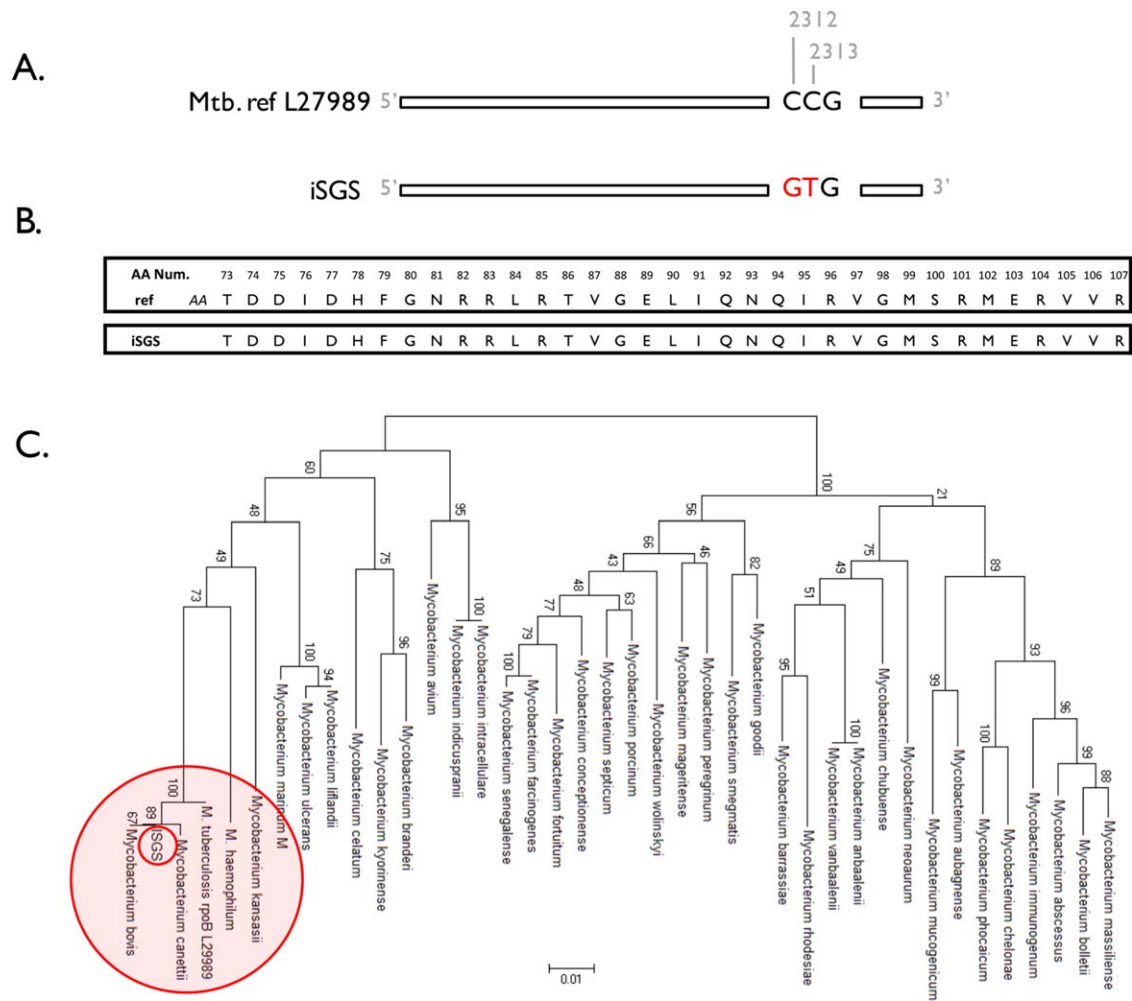


Fig. 2. Sanger sequencing of *Mycobacterium* species. Sanger sequencing of the *mycobacterium rpoB* gene in iSGS scar demonstrating 99% positional identity with *MtbC* in eight of 20 iSGS samples. (A) Seven of the eight positive samples demonstrated two identical synonymous substitutions at positions 2312 and 2313. (B) Predicted identical *rpoB* amino acid sequence in *MtbC* and iSGS specimens. Analysis of *rpoB* DNA sequences from 29 *Mycobacterium* species and from patients with iSGS showing distinct clustering of iSGS samples. Phylograms based on nucleotide alignments were generated with HKY85 distances matrices using Paup 4.0b10 (Sinauer Associates, Sunderland, MA). (C) Bootstrap values > 50 (based on 500 replicates) are represented at each node. The branch length index is represented below the phylogram. iSGS = idiopathic subglottic stenosis; *MtbC* = *mycobacterium tuberculosis complex*.

The use of antigen-specific immune responses to microbial antigens has also been utilized to identify novel infectious agents, including Sin Nombre virus in hantavirus pulmonary syndrome,³⁷ as well as a previously unknown coronavirus in severe acute respiratory syndrome^{38,39} and *Mycobacterium* in sarcoidosis.^{28,40} Peripheral blood mononuclear cells from iSGS patients that are stimulated *ex vivo* with mycobacterial virulence factor ESAT-6 demonstrate a pronounced IFN γ response. This finding suggests that, despite negative culture results from iSGS specimens, mycobacterial antigens induce T-cell-specific responses in the blood of iSGS patients at similar frequencies to those of tuberculosis subjects.²⁸ The observation of a pronounced cellular immune response to *Mycobacterium* EAST-6 antigens in all 10 iSGS patients tested strongly supports the results from our molecular and protein analysis of iSGS scar.

The inability to identify mycobacterial microorganisms by routine histologic staining or to culture microor-

ganisms from pathologic tissues provides caution to the establishment of a causative role for infectious agents in iSGS pathogenesis. However, based on prior microbiological experience with fastidious mycobacteria, there are several explanations for the failure to detect microbial species in iSGS in the initial reports of the disease: The bacteria may be present in quantities below the detection of histologic staining.⁴¹ Alternatively, the agent may have an ultraslow growth pattern that necessitates incubation periods much longer than the standard 6 weeks that cultures are held for isolation of *Mycobacterium tuberculosis*, which is similar to the time needed for isolation of *M. ulcerans*.⁴² Conversely, iSGS pathogenesis may reflect an immune response to infectious antigens and might not be dependent on actively replicating organisms, which is similar to the hypersensitivity pneumonitis that is induced by *Mycobacterium avium*.⁴³

An association between *Mycobacterium* and iSGS immunopathogenesis is supported by the detection of

mycobacterial proteins and nucleic acids in iSGS scar, as well as local and peripheral cellular immune responses to mycobacterial antigens in iSGS subjects. However, it remains unresolved whether the identified mycobacterial constituents drive disease or whether inflammation per se creates a niche for the outgrowth of specific bacteria. It should be noted, however, that tracheal stenosis arising after intubation (iLTS; which also possess an inflammatory tissue phenotype in the airway) appears in our cohort to have a much lower percentage of patients with detected *Mycobacterium*. Given the disease rarity, these results will require confirmation in larger cohorts pooled from multiple institutions.

The presence of *Mycobacterium* within iSGS scar is particularly striking in light of proven association of *Mycobacterium* with otherwise healthy, older white females (the Lady Windermere syndrome).⁴⁴ The characteristics of these patients (women without immunocompromise or underlying chronic lung disease and proven pulmonary *Mycobacterium* infection) closely mirror the iSGS population. Lady Windermere patients are predominantly Caucasian (86%) women (81%) presenting in their mid-sixties. The dramatic demographic similarities of the two diseases (NTM pulmonary infection/Lady Windermere syndrome and iSGS) offers clinical precedent for a pathogenic role for *Mycobacterium* in the development or progression of iSGS.

Although our results demonstrate *Mycobacterium* species within the tracheal scar of iSGS patients, the role of host genetics to iSGS pathogenesis has not yet been explored. Interestingly, strong alternate evidence links host genotype to mycobacterial susceptibility via the IL-23/IL-17A axis. Molecular analysis of patients suffering from Mendelian susceptibility to mycobacterial disease has implicated polymorphisms in both the ligand (IL-12B)^{45,46} and receptor (IL-12R β 1)^{47,48} responsible for IL-17A activation. Similarly, although iSGS affects women nearly exclusively, the influence of estrogen on disease initiation and recurrence is unknown. Estrogen has been shown to directly drive IL-23/IL-23R signaling and increase IL-17A production in severe asthma.⁴⁹ The role of estrogen in promoting mycobacterial colonization/infection, or its role in accelerating the host response to pathogen, are questions meriting future study.

CONCLUSION

Although iSGS has long been considered strictly an anatomic abnormality requiring a surgical remedy, we offer the first evidence that the disease may represent a manifestation of altered local microbial flora coupled to a pathologic host inflammatory response. We demonstrate through multiple distinct approaches, a unique association of mycobacterial species and iSGS airway mucosa. Together with prior reports demonstrating significantly upregulated local IL-17A, evidence of *Mycobacterium* species within tracheal scar offers new avenues for therapeutic intervention in iSGS patients. Several established reagents are available to inhibit the IL-17A pathway.^{50–52} Alternatively, multiple drugs are available targeting *Mycobacterium* species. Interestingly,

limited cases series supports a clinical benefit for one of these reagents in iSGS patients.¹ The benefit of IL-17A inhibition in the absence of pathogen control is unclear; thus, future clinical trials could test the clinical response of immunomodulation in combination with antibacterial therapy. Therefore, the implications this work may extend beyond the confines of iSGS to other disease arising at the interface of pathogen and host inflammatory response.

Acknowledgment

This was a North American Airway Collaborative TS-04 study.

AUTHOR CONTRIBUTIONS

A.G. designed and performed experiments, analyzed data, and wrote the article; N.K. analyzed data; M.M. designed and performed experiments; D.N. designed and performed experiments; B.R. aided in experimental design; J.D., E.S.E., E., J.K., A.H., analyzed data, preformed critical scientific review; G.G. aided in experimental design; L.Y. analyzed data; J.R. conducted experiments; J.N. aided in experimental design; C.W. aided in experimental design; D.F. aided in experimental design, statistical analysis; C.S. conducted experiments; K.J. conducted experiments; T.M. aided in experimental design, data analysis, review of article; T.B. aided in experimental design, experiments, data analysis, review of article; J.G. conducted experiments; W.D. aided in experimental design, experiments, data analysis, review of article.

BIBLIOGRAPHY

1. Gelbard A, Donovan DT, Ongkasuwan J, et al. Disease homogeneity and treatment heterogeneity in idiopathic subglottic stenosis. *Laryngoscope* 2015. doi: 10.1002/lary.25708. Epub ahead of print.
2. Mark EJ, Meng F, Kradin RL, Mathisen DJ, Matsubara O. Idiopathic tracheal stenosis: a clinicopathologic study of 63 cases and comparison of the pathology with chondromalacia. *Am J Surg Pathol* 2008;32:1138–1143.
3. Wang H, Wright CD, Wain JC, Ott HC, Mathisen DJ. Idiopathic subglottic stenosis: factors affecting outcome after single-stage repair. *Ann Thorac Surg* 2015;100:1804–1811.
4. Nouraei SM, Franco RA, Dowdall JR, et al. Physiology-based minimum clinically important difference thresholds in adult laryngotracheal stenosis. *Laryngoscope* 2014;124:2313–2320.
5. Brandenburg JH. Idiopathic subglottic stenosis. *Trans Am Acad Ophthalmol Otolaryngol* 1972;76:1402–1406.
6. Davies DE. The role of the epithelium in airway remodeling in asthma. *Proc Am Thorac Soc* 2009;6:678–682.
7. Holgate ST, Davies DE, Lackie PM, Wilson SJ, Puddicombe SM, Lordan JL. Epithelial-mesenchymal interactions in the pathogenesis of asthma. *J Allergy Clin Immunol* 2000;105:193–204.
8. Levine SJ. Bronchial epithelial cell-cytokine interactions in airway inflammation. *J Invest Med* 1995;43:241–249.
9. Tanjore H, Xu XC, Polosukhin VV, et al. Contribution of epithelial-derived fibroblasts to bleomycin-induced lung fibrosis. *Am J Respir Crit Care Med* 2009;180:657–665.
10. Abreu NA, Nagalingam NA, Song Y, et al. Sinus microbiome diversity depletion and *Corynebacterium tuberculostearicum* enrichment mediates rhinosinusitis. *Sci Transl Med* 2012;4:151ra124.
11. Lawson WE, Crossno PF, Polosukhin VV, et al. Endoplasmic reticulum stress in alveolar epithelial cells is prominent in IPF: association with altered surfactant protein processing and herpesvirus infection. *Am J Physiol Lung Cell Mol Physiol* 2008;294:L1119–1126.
12. Hilty M, Burke C, Pedro H, et al. Disordered microbial communities in asthmatic airways. *PloS One* 2010;5:e8578.
13. Erb-Downward JR, Thompson DL, Han MK, et al. Analysis of the lung microbiome in the “healthy” smoker and in COPD. *PloS One* 2011;6:e16384.
14. Blainey PC, Milla CE, Cornfield DN, Quake SR. Quantitative analysis of the human airway microbial ecology reveals a pervasive signature for cystic fibrosis. *Sci Transl Med* 2012;4:153ra130.

15. Drake WP, Newman LS. Mycobacterial antigens may be important in sarcoidosis pathogenesis. *Curr Opin Pulm Med* 2006;12:359–363.
16. Frank DN, St Amand AL, Feldman RA, Boedeker EC, Harpaz N, Pace NR. Molecular-phylogenetic characterization of microbial community imbalances in human inflammatory bowel diseases. *Proc Natl Acad Sci U S A* 2007;104:13780–13785.
17. Hauth JC, Goldenberg RL, Andrews WW, DuBard MB, Copper RL. Reduced incidence of preterm delivery with metronidazole and erythromycin in women with bacterial vaginosis. *N Engl J Med* 1995;333:1732–1736.
18. Gupta K, Stapleton AE, Hooton TM, Roberts PL, Fennell CL, Stamm WE. Inverse association of H2O2-producing lactobacilli and vaginal *Escherichia coli* colonization in women with recurrent urinary tract infections. *J Infect Dis* 1998;178:446–450.
19. Lemon KP, Klepac-Ceraj V, Schiffer HK, Brodie EL, Lynch SV, Kolter R. Comparative analyses of the bacterial microbiota of the human nostril and oropharynx. *MBio* 2010;1. pii: e00129-10. doi: 10.1128/mBio.00129-10.
20. Costello EK, Lauber CL, Hamady M, Fierer N, Gordon JI, Knight R. Bacterial community variation in human body habitats across space and time. *Science* 2009;326:1694–1697.
21. Gelbard A, Katsantonis NG, Mizuta M, et al. Idiopathic subglottic stenosis is associated with activation of the inflammatory IL-17A/IL23 axis. *Laryngoscope* 2016.
22. Nouraei SA, Sandhu GS. Outcome of a multimodality approach to the management of idiopathic subglottic stenosis. *Laryngoscope* 2013;123:2474–2484.
23. Verhelst R, Verstraelen H, Claeys G, et al. Cloning of 16S rRNA genes amplified from normal and disturbed vaginal microflora suggests a strong association between *Atopobium vaginae*, *Gardnerella vaginalis* and bacterial vaginosis. *BMC Microbiol* 2004;4:16.
24. Yuan S, Cohen DB, Ravel J, Abdo Z, Forney LJ. Evaluation of methods for the extraction and purification of DNA from the human microbiome. *PLoS One* 2012;7:e33865.
25. Wang F, Flanagan J, Su N, et al. RNAscope: a novel in situ RNA analysis platform for formalin-fixed, paraffin-embedded tissues. *J Mol Diagn* 2012;14:22–29.
26. Drake WP, Pei Z, Pride DT, Collins RD, Cover TL, Blaser MJ. Molecular analysis of sarcoidosis tissues for *Mycobacterium* species DNA. *Emerg Infect Dis* 2002;8:1334–1341.
27. Parekh VV, Wu L, Boyd KL, et al. Impaired autophagy, defective T cell homeostasis, and a wasting syndrome in mice with a T cell-specific deletion of *Vps34*. *J Immunol* 2013;190:5086–5101.
28. Drake WP, Dhason MS, Nadaf M, et al. Cellular recognition of *Mycobacterium tuberculosis* ESAT-6 and KatG peptides in systemic sarcoidosis. *Infect Immun* 2007;75:527–530.
29. Koulenti D, Lisboa T, Brun-Buisson C, et al. Spectrum of practice in the diagnosis of nosocomial pneumonia in patients requiring mechanical ventilation in European intensive care units. *Crit Care Med* 2009;37:2360–2368.
30. Takiff HE, Salazar L, Guerrero C, et al. Cloning and nucleotide sequence of *Mycobacterium tuberculosis gyrA* and *gyrB* genes and detection of quinolone resistance mutations. *Antimicrob Agents Chemother* 1994;38:773–780.
31. Carlisle J, Evans W, Hajizadeh R, et al. Multiple *Mycobacterium* antigens induce interferon-gamma production from sarcoidosis peripheral blood mononuclear cells. *Clin Exp Immunol* 2007;150:460–468.
32. Lockhart E, Green AM, Flynn JL. IL-17 production is dominated by gamma-delta T cells rather than CD4 T cells during *Mycobacterium tuberculosis* infection. *J Immunol* 2006;177:4662–4669.
33. Basile JI, Geffner LJ, Romero MM, et al. Outbreaks of *Mycobacterium tuberculosis* MDR strains induce high IL-17 T-cell response in patients with MDR tuberculosis that is closely associated with high antigen load. *J Infect Dis* 2011;204:1054–1064.
34. Grillo HC, Mark EJ, Mathisen DJ, Wain JC. Idiopathic laryngotracheal stenosis and its management. *Ann Thorac Surg* 1993;56:80–87.
35. Relman DA, Loutit JS, Schmidt TM, Falkow S, Tompkins LS. The agent of bacillary angiomatosis. An approach to the identification of uncultured pathogens. *N Engl J Med* 1990;323:1573–1580.
36. Relman DA, Schmidt TM, MacDermott RP, Falkow S. Identification of the uncultured bacillus of Whipple's disease. *N Engl J Med* 1992;327:293–301.
37. Nichol ST, Spiropoulou CF, Morzunov S, et al. Genetic identification of a hantavirus associated with an outbreak of acute respiratory illness. *Science* 1993;262:914–917.
38. Rota PA, Oberste MS, Monroe SS, et al. Characterization of a novel coronavirus associated with severe acute respiratory syndrome. *Science* 2003;300:1394–1399.
39. Ksiazek TG, Erdman D, Goldsmith CS, et al. A novel coronavirus associated with severe acute respiratory syndrome. *N Engl J Med* 2003;348:1953–1966.
40. Song Z, Marzilli L, Greenlee BM, et al. Mycobacterial catalase-peroxidase is a tissue antigen and target of the adaptive immune response in systemic sarcoidosis. *J Exp Med* 2005;201:755–767.
41. David HL. Bacteriology of the Mycobacterioses. Atlanta, GA: US Dept. of Health, Education, and Welfare, Public Health Service, and Center for Disease Control, 1978.
42. Portaels F, Agular J, Fissette K, et al. Direct detection and identification of *Mycobacterium ulcerans* in clinical specimens by PCR and oligonucleotide-specific capture plate hybridization. *J Clin Microbiol* 1997;35:1097–1100.
43. Hanak V, Kalra S, Aksamit TR, Hartman TE, Tazelaar HD, Ryu JH. Hot tub lung: presenting features and clinical course of 21 patients. *Respir Med* 2006;100:610–615.
44. Prince DS, Peterson DD, Steiner RM, et al. Infection with *Mycobacterium avium* complex in patients without predisposing conditions. *N Engl J Med* 1989;321:863–868.
45. Picard C, Fieschi C, Altare F, et al. Inherited interleukin-12 deficiency: IL12B genotype and clinical phenotype of 13 patients from six kindreds. *Am J Hum Genet* 2002;70:336–348.
46. Altare F, Lammas D, Revy P, et al. Inherited interleukin 12 deficiency in a child with bacille Calmette-Guerin and *Salmonella enteritidis* disseminated infection. *J Clin Invest* 1998;102:2035–2040.
47. Fieschi C, Dupuis S, Catherinet E, et al. Low penetrance, broad resistance, and favorable outcome of interleukin 12 receptor beta1 deficiency: medical and immunological implications. *J Exp Med* 2003;197:527–535.
48. de Beaucoudrey L, Samarina A, Bustamante J, et al. Revisiting human IL-12Rbeta1 deficiency: a survey of 141 patients from 30 countries. *Medicine (Baltimore)* 2010;89:381–402.
49. Newcomb DC, Cephus JY, Boswell MG, et al. Estrogen and progesterone decrease let-7f microRNA expression and increase IL-23/IL-23 receptor signaling and IL-17A production in patients with severe asthma. *J Allergy Clin Immunol* 2015;136:1025–1034.e11.
50. Silva JC, Mariz HA, Rocha LF Jr, et al. Hydroxychloroquine decreases Th17-related cytokines in systemic lupus erythematosus and rheumatoid arthritis patients. *Clinics (Sao Paulo)* 2013;68:766–771.
51. Griffiths CE, Reich K, Lebwohl M, et al. Comparison of ixekizumab with etanercept or placebo in moderate-to-severe psoriasis (UNCOVER-2 and UNCOVER-3): results from two phase 3 randomised trials. *Lancet* 2015;386:541–551.
52. Lebwohl M, Strober B, Menter A, et al. Phase 3 studies comparing Brodalumab with Ustekinumab in psoriasis. *N Engl J Med* 2015;373:1318–1328.